Contents lists available at ScienceDirect

EBioMedicine

Research paper

Persistent lentivirus infection induces early myeloid suppressor cells expansion to subvert protective memory CD8 T cell response☆,☆☆

Li Liu[a,b,#,*], Qingqing Lin[a,#], Jie Peng[a,#], Jun Fang[a], Zhiwu Tan[a], Hangying Tang[a], Kayi Kwan[a], Kenji Nishiura[a], Jianguo Liang[a], Hauyee Kwok[a], Zhenglong Du[a], Jiaze Sun[a], Kang Liu[c], Kwok-Yung Yuen[a], Hui Wang[b,*], Zhiwei Chen[a,b,*]

[a] AIDS Institute and Department of Microbiology, State Key Laboratory of Infectious Diseases, Li Ka Shing Faculty of Medicine, The University of Hong Kong, 21 Sassoon Road, Hong Kong SAR, P.R. China
[b] HKU-AIDS Institute Shenzhen Research Laboratory and AIDS Clinical Research Laboratory, Shenzhen Key Laboratory of Infection and Immunity, Shenzhen Key Clinical Department of Emerging Infectious Diseases, Shenzhen Third People's Hospital, Shenzhen, P.R. China
[c] Department of Microbiology and Immunology, Columbia University Medical Center, New York, NY, United States

A B S T R A C T

Background: Memory CD8^{+} T cell responses play an essential role in protection against persistent infection. However, HIV-1 evades vaccine-induced memory CD8^{+} T cell response by mechanisms that are not fully understood.
Methods: We analyzed the temporal dynamics of CD8^{+} T cell recall activity and function during EcoHIV infection in a potent PD1-based vaccine immunized immunocompetent mice.
Findings: Upon intraperitoneal EcoHIV infection, high levels of HIV-1 GAG-specific CD8^{+} T lymphocytes recall response reduced EcoHIV-infected cells significantly. However, this protective effect diminished quickly after seven days, followed by a rapid reduction of GAG-specific CD8^{+} T cell number and activity, and viral persistence. Mechanistically, EcoHIV activated dendritic cells (DCs) and myeloid cells. Myeloid cells were infected and rapidly expanded, exhibiting elevated PD-L1/-L2 expression and T cell suppressive function before day 7, and were resistant to CD8^{+} T cell-mediated apoptosis. Depletion of myeloid-derived suppressor cells (MDSCs) reduced EcoHIV infection and boosted T cell responses.
Interpretation: This study provides an overview of the temporal interplay of persistent virus, DCs, MDSCs and antigen-specific CD8^{+} T cells during acute infection. We identify MDSCs as critical gatekeepers that restrain antiviral T cell memory responses, and highlight MDSCs as an important target for developing effective vaccines against chronic human infections.
Funding: Hong Kong Research Grant Council (T11−709/18-N, HKU5/CRF/13G), General Research Fund (17122915 and 17114114), Hong Kong Health and Medical Research Fund (11100752, 14130582, 16150662), Grant RGC-ANR A-HKU709/14, the San-Ming Project of Medicine (SZSM201512029), University Development Fund of the University of Hong Kong and Li Ka Shing Faculty of Medicine Matching Fund to HKU AIDS Institute.

1. Introduction (7406)

Human immunodeficiency virus type one (HIV-1) is one of the most devastating infectious agents existing worldwide for the past 37 years. There were approximately 25.7 million people living with HIV at the end of 2018 with 1.1 million people becoming newly infected in 2017 globally. The induction of protective T cell immunity is a prerequisite for the durable control of HIV-1 [1,2]. However, host immunosuppression is a hallmark of HIV-1 and other persistent viral infections. Despite initial antiviral immune activity, persistent viruses eventually evade host immune responses [1, 3] and induce expansion of immune regulatory cells in the host that suppress antiviral T cell immunity [4, 5], facilitating persistent chronic infection [6-8]. This

Research in context

Evidence before this study

Host immunosuppression is a hallmark of HIV-1 and other persistent viral infections. Persistent viruses evade host immune responses and induce expansion of immune regulatory cells in the host that suppress antiviral T cell immunity, facilitating persistent chronic infection. The dynamic of the immunosuppressive response and how this response affects memory T cell recall responses and function driven by prior vaccination remains largely unclear.

Added value of this study

This study provides an overview of the temporal interplay of a persistent virus, DCs, MDSCs, and antigen-specific CD8$^+$ T cells during acute infection. We demonstrated that despite initial high levels of viral-specific CD8$^+$ T lymphocytes recall response, persistent viruses evade host immune responses through infection of MDSC, and induction of quick MDSC expansion. MDSCs suppressed T cell function within 7 days post infection and were resistant to CD8$^+$ T cell-mediated apoptosis. Depletion of MDSCs reduced infection and boosted T cell function in vivo.

Implications of all the available evidence

MDSCs are critical gatekeepers that restrain antiviral T cell memory responses and may serve as an important target for developing effective vaccines against chronic human infections.

immunosuppression is also seen as a host adaptation that enables long-term survival and coexistence with the pathogen, because individuals with genetic ablation of core immunosuppressors often die after infection [9]. The dynamics of the immunosuppressive response and how this host adaptation affects memory T cell recall responses and function driven by prior vaccination remains largely unclear. However, understanding these mechanisms will be critical for the design of an effective vaccine or immunotherapy against HIV-1 and other chronic diseases.

CD8$^+$ T cells play a critical role in vaccine-mediated protection against a number of viral and bacterial pathogens [10,11]. After vaccination, naive CD8$^+$ T cells are primed and undergo a rapid expansion phase to generate large numbers of effector cells for pathogen elimination. Subsequently, a contraction period takes place in which most effector cells are eliminated, leaving a small, long-lived memory cell pool [12]. When individuals encounter the vaccine-related pathogen, antigen-specific memory T cells can respond swiftly with robust proliferation and upregulation of effector function. Analysis of cellular requirements for generating a memory CD8$^+$ T cell recall response during acute viral infection has suggested a critical role for dendritic cells (DCs) and CD4$^+$ helper T cells. Activation of memory T cells in response to systemic or localized infection is predominantly dependent on DCs, and the number of responding memory CD8$^+$ T cells is profoundly decreased during the recall response to various acute infections in DC-depleted mice [13]. However, the dependence of CD8$^+$ T cell recall response on CD4$^+$ T cells remains controversial. In some cases, CD4$^+$ T cells assist proliferative CD8$^+$ T cell recall responses, whereas in other situations, CD4$^+$ T cells appear to be dispensable for the secondary response [14-16].

During chronic lentiviral infection, both CD4$^+$ and CD8$^+$ T cell responses are suppressed by various mechanisms, and these cells subsequently acquire an exhausted phenotype characterized by

upregulation of inhibitory molecules such as PD-1, Tim3 or vista, and reduced production of effector molecules such as IFN-γ, TNF, granzymes, and perforin [5,8,17]. Myeloid-derived suppressor cells (MDSCs) have recently emerged as a major suppressor of immune responses in chronic infection and tumors [18-22]. MDSCs are immature myeloid cells that are induced and accumulated during persistent viral infection [23,24], and suppress both innate and adaptive immune responses through many mechanisms. For example, they produce arginase 1 (ARG1), indoleamine 2,3-dioxygenase (IDO), inducible nitric oxide synthase (NOS2), NADPH oxidase and immunosuppressive cytokines to suppress DC, CTLs and natural killer (NK) cell function, deplete nutrients required by lymphocytes, which causes proliferative arrest of antigen-activated T cells, and expands CD4$^+$ CD25$^+$ FoxP3$^+$ regulatory T cells (Tregs) [19,25-28].

We recently developed a potent sPD1-p24$_{fc}$/EP DNA DC-targeting vaccine, which consistently induces a high frequency of durable HIV-1 GAG-specific CD8$^+$ T lymphocytes [29]. Following vaccination, we detected up to 21% of p24 tetramer-positive CD8$^+$ T cells in the mouse spleen, and these exhibited broad reactivity, polyfunctionality and cytotoxicity. This model vaccine was subsequently employed to achieve complete and long-lasting protection against lethal mesothelioma challenge by CD8$^+$ T cells in immunocompetent BALB/c mice [18]. We have now utilized this vaccine to analyze the secondary T cell immune response to a persistent lentivirus, and the correlation of the recall responses in prevention and curing of persistent infection. We adopted the lentiviral model of EcoHIV, which establishes persistent infection in immunocompetent BALB/c mice [30,31]. Considering that immunosuppression was typically observed during chronic infection [20,24,32], we reasoned that efficient reactivation of large numbers of memory CD8$^+$ T cells with broad reactivity and polyfunctionality might be sufficient to rapidly eliminate infected cells before the induction of immunosuppressive cells, thus preventing persistent infection. However, our results indicated that despite effective initial memory CD8$^+$ T cell reactivation, there was a rapid expansion of MDSCs within 7 days post-infection (dpi), which profoundly subverted the memory CD8$^+$ T cell response both in terms of number and function at a very early stage of infection, resulted in viral persistence.

2. Materials and methods

2.1. Mice and viruses

6- to 8-week- old female BALB/c (Charles River Laboratory), OT-I (Rag1/2+/+) mice were maintained under specific-pathogen-free conditions in the Laboratory Animal Unit. EcoHIV strains from David Volsky of Columbia University were grown and quantified, as described previously [30].

2.2. Mouse immunization and challenge

Construction of the DNA vaccines sPD1-p24fc and p24fc and the immunization procedure were previously described [18,29]. Mice received three DNA immunizations by intramuscular injection with EP given every three weeks at a dose of 100 μg per mouse. After the final immunization, the mice were challenged with EcoHIV via i.p. route and subsequently sacrificed at 1, 2, 3, or 12 weeks, after which sera and splenocytes were collected for analysis.

2.3. qPCR quantitation of proviral load

qPCR quantitation of total HIV DNA in EcoHIV-infected mice and DNA standardization was conducted as previously described [33] with forward primer 5'-CCCTCAGATGCTGCATATAAGC-3', and reverse primer 5'−GCACTCAAGGCAAGCTTTATTG−3' for LTR. DNA content was standardized by amplification of murine β globin with forward

primer 5′−GGTTTCCTTCCCCTGGCTAT−3′ and reverse primer 5′−CGCTTCCCCTTTCCTTCTG−3′.

2.4. Evaluation of gag p24-specific t cell responses

Evaluation of IFNγ−producing T cells were conducted by ELISpot assay (Millipore) as previously described [18,29]. Briefly, splenocytes were stimulated with 10 μg/mL of HIV-1 p24 peptide or peptide pools in vitro (NIH, catalog no. 8117). The peptide pools were generated by dividing 59 GAG p24 peptides into three pools. Each pool contains 19−20 peptides spanning amino acids 1−87 (pool 1), 77−167 (pool 2), and 157−231 (pool 3). The final concentration of each peptide in three pools is 2 μg/ml. Peptide GAG A-I (AMQMLKDTI) is specific to CD8+ T cells, whereas peptide GAG 26 (TSNPPIPVGDIYKRWIILGL) is specific to CD4+ T cells. Cells stimulated with 500 ng/ml phorbol 12-myristate 13-acetate (PMA; Sigma-Aldrich) plus 1 μg/ml calcium ionomycin or left in media only served as positive and negative controls, respectively. Cells were incubated at 37 °C, and 5% CO$_2$, for 20 h. ImmunoSpot analyzer (Thermo Fisher Scientific) was used to detect the spots. Tetramer-positive CD8$^+$ T cells were detected using MHC class I tetramer H2d-Kd-AMQMLKDTI (Beckman Coulter).

2.5. T cell proliferation assay

Splenocytes isolated from BALB/c mice were labeled with 1 μM CFSE (Invitrogen) at 10^7 cells/ml in PBS for 10 min in a 37 °C water bath, and cultured in the presence of HIV-1 GAG p24 peptide pools (2 μg/ml), or with anti-CD28 (2 μg/ml) and anti-CD3 (0.1 μg/ml) antibodies. Cells were collected after five days of coculture, and stained with fluorochrome-conjugated antibodies. Data were acquired using a FACSAria III flow cytometer (BD Biosciences), and analyzed with FlowJo softwarev10 (TreeStar Inc.).

2.6. Antigen-presenting cell functional assays

Total DCs and CD8$^+$ T cells were purified from the mice's spleens by anti-CD11c$^+$ microbeads (Biolegend) and immunomagnetic beads (Invitrogen), respectively. Total DC and CD8$^+$ T cell populations were determined as >95% pure by flow cytometry. Purified DCs were cultured with 10^5 CFSE-labeled CD8$^+$ OT-I T cells at a ratio of 1:1 with or without the presence of SIINFEKL peptide (GenScript) for 5 days, and then were stained with fluorochrome-conjugated antibodies and analyzed on a BD Aria III flow cytometer (BD Biosciences).

2.7. T cell suppression assay

Total MDSCs were enriched from the spleens of day 14 EcoHIV-infected mice via MACS beads. The average purity of monocytic populations from three experiments was >90%. Myeloid cells were added to 10^5 CFSE-labeled splenocytes from sPD1-p24fc/EP DNA vaccinated and unchallenged mice, and cultured for 5 days with p24 peptide pools or CD28/CD3 antibodies before evaluating proliferation.

2.8. MDSC isolation and culture

MDSCs were isolated from spleens of EcoHIV-infected BALB/c mice using the Miltenyi Biotech MDSC Isolation Kit, according to the manufacturer's protocols. The purity of MDSCs was greater than 95% as determined by flow cytometry. To assess CD8$^+$ T cell-mediated apoptosis, MDSCs and freshly isolated CD8$^+$ T cells were co-cultured at MDSC-to-CD8$^+$ T cell ratios of 1:1, 1:2, and 1:5 in a 37 °C incubator for 24 hrs before being subjected to analysis of active caspase-3.

2.9. Myeloid cell depletion in vivo

Mice immunized and infected with EcoHIV were given intraperitoneal injections of 100 μg of anti-Gr1 (RB6−8C5) or a rat IgG2b isotype control (LTF-2) (Bio X Cell), at 7, 9, and 11 dpi. Blood, peritoneum macrophages and spleen were collected on day 14.

2.10. Double immunofluorescence staining on paraffin sections

The samples were de-paraffinized and rehydrated, as previously described [34]. After 30 min blocking with normal goat serum at room temperature, samples were incubated with primary antibody at 4 °C overnight, followed by an Alexa448/568/647-conjugated secondary antibody for 1 h at room temperature. primary antibodies used in this study include: p24 (DAKO, M085701−1; 1/5 dilution); CD3 (DAKO, A0452; 1:50 dilution); Gr1 (Abcam); F4/80 (Biolegend, 123,102; 1/50 dilution). To differentiate between individual cells, samples were incubated with 1 μg/ml Hoechst 33,258 (Thermo Fisher Scientific) for 5 min at room temperature, followed by rinsing with water.

2.11. Confocal microscopy

A Carl Zeiss LSM 700 confocal microscope (Carl Zeiss, Oberkochen, Germany) was used to perform Confocal microscopy. ZEN (Zeiss) was used to assign colors, which were collected simultaneously: Alexa 568 (Thermo Fisher Scientific) and HNPP/Fast Red, which fluoresce red when excited by a 568-nm laser; Alexa 488 (Thermo Fisher Scientific), which fluoresces green when excited at 488 nm; Alexa 647 (Thermo Fisher Scientific), which fluoresces cyan when excited at 647 nm; and the differential interference contrast (DIC) image, which is in grayscale.

2.12. Statistical analysis

A two-tailed Student t-test was performed to determine statistical significance between different groups. An additional test using the Bonferroni-Holms method was performed when multiple comparisons being made. P-value of less than 0.05 was considered to be statistically significant. Data are presented as the mean values $\pm$ standard error (s.e.m.).

2.13. Study approval

All experimental procedures were approved by the University of Hong Kong Committee on the Use of Live Animals in Teaching and Research (CULATR 3638−15).

3. Results

3.1. EcoHIV established persistent infection and induced immune suppression in immune competent mice

EcoHIV is a chimeric HIV strain that have been modified to infect mice by replacing HIV env (1405 bp) with the coding region of the ecotropic envelope gp80 of ecotropic murine leukemia virus (MLV) in the backbone of HIV-1 clade B (Fig. 1a). All HIV-1 cis-regulatory elements were preserved, and expression of the entire construct was driven by the HIV-1 LTR. It is capable to infect, replicate and persist in macrophages and CD4+ T cells of infected mice [30,31], and has been used in several HIV-1 vaccine and therapeutic studies [30,33,35,36]. To study if EcoHIV infection leads to an immunosuppressive environment, we injected a group of BALB/c mice with 400 ng p24 EcoHIV intraperitoneally (i.p.), performed kinetic analysis of proviral load in blood for up to 12 weeks, and measured expression of the inhibitory molecules PD-1 and Tim3 on T cells, as well as numbers of Treg cells and MDSCs in the lymph node or spleen at 12 weeks post infection (wpi). Successful establishment of persistent infection was
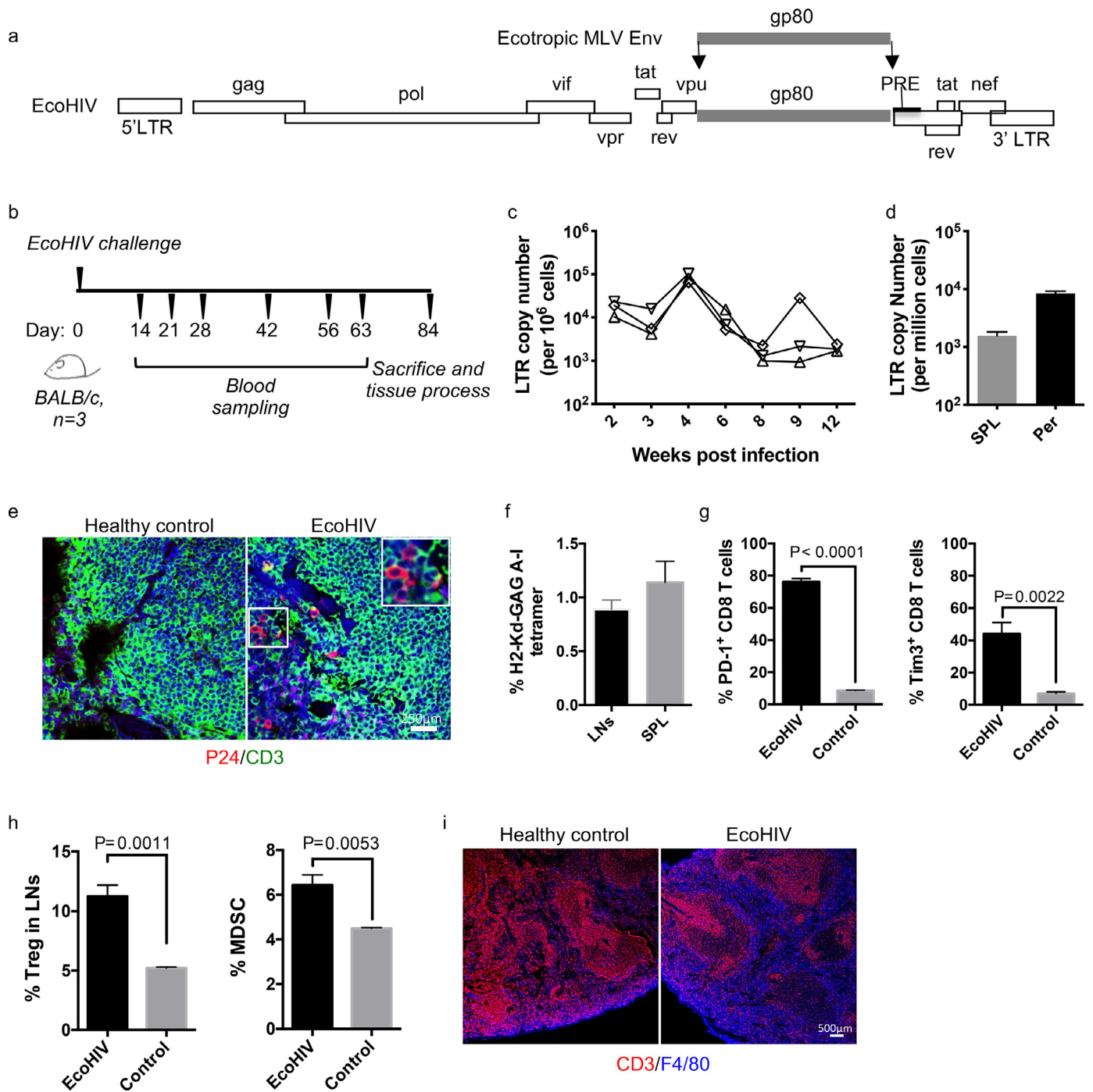
Fig. 1. Persistent EcoHIV infection and immunosuppression in immunocompetent BALB/c mice. a. Schematic map of EcoHIV. HIV-1 env (1405 bp) was replaced by the coding region of the ecotropic envelope gp80 of MLV. All HIV-1 cis-regulatory elements were preserved, and expression of the entire construct was driven by the HIV-1 LTR. b. Experimental schedule. Mice were inoculated once with EcoHIV, after which blood was collected every 7 to 14 days. Mice were sacrificed at 84 days post-infection (dpi). c. Viral burden in the blood after EcoHIV infection. d. Comparison of viral burden in splenocytes (SPL) and peritoneal macrophages (Per) at 84 dpi. Viral burdens were determined by qPCR, with data normalized based on cellular β-globin levels. e. Distribution of p24$^+$ (red) cells in spleens at 84 dpi based on immunohistochemistry (IHC) in healthy control (left) and EcoHIV-infected (right) mice. f. Similar levels of p24-specific CD8$^+$ T cell responses were detected in the lymph node (LNs) and spleen (SPL) based on H2-Kd-GAG A-I tetramer staining. g. Percentage of PD-1- (left) and Tim3- (right) expressing CD8$^+$ T cells in the spleen at 84 dpi based on flow cytometry analysis. h. Percentage of regulatory CD4$^+$ T cells (Treg) in lymph nodes (left) and MDSC in spleen (right) were determined at 84 dpi by flow cytometry analysis. i. IHC shows T lymphopenia in EcoHIV-infected spleens compared to healthy controls at 84 dpi. Data represent three independent experiments with three mice per group and with error bars representing the SEM. A two-tailed Student t-test was used to determine statistical significance between different groups.

consistently confirmed by the presence of provirus in PBMCs, measured every 1 or 2 weeks for 12 weeks (Fig. 1b and 1c). At week 12, mice were sacrificed, and provirus copies were detectable in spleen and peritoneal macrophages from all mice tested (Fig. 1d). Viral replication was determined by detection of viral protein p24 in spleens of EcoHIV-infected mice by immunohistochemistry (IHC) staining using an anti-p24 antibody (Fig. 1e). Persistent infection induced a p24-specific CD8$^+$ T cell response, and up to 1.06% and 1.53% of CD8$^+$ T cells in lymph nodes and spleens, respectively, were positive for H2-Kd-GAG A-I tetramer binding (Fig. 1f and Fig. S1).

We then investigated whether EcoHIV induced immunosuppression at week 12 by measuring proportions of CD4$^+$ and CD8$^+$ T cells,

Treg cells (CD4$^+$CD25$^+$Foxp3$^+$) and MDSCs (CD11b$^+$Gr-1$^+$) and expression of PD-1 and Tim-3 on CD8$^+$ T cells in mouse lymph nodes and spleens. We did not observe significant decrease of frequencies of the CD4$^+$ or CD8$^+$ T cells. However, EcoHIV infection led to up-regulation of PD-1 and Tim-3 on CD8$^+$ T cells (Fig. 1g), and expansion of MDSCs in the spleen and Treg cells in the lymph nodes (Fig. 1h and Fig. S1). Lymphoid architecture is integral to induction and maintenance of immune responses, and EcoHIV infection resulted in slight splenic disorganization at 12 wpi, with a higher proportion of F4/80$^+$ myeloid cells and a corresponding loss of T cells (Fig. 1i), consistent with previous reports of other chronic infection, such as lymphocytic choriomeningitis virus (LCMV) [24]. These results suggest that although EcoHIV does not induce canonical immunosuppression as shown in patients with AIDS with significant loss of CD4 T-cells, it establishes persistent infection and induces immune suppression in chronically infected mice.

3.2. Prophylactic vaccination-mediated virus clearance was restrained by day 7

After establishing the EcoHIV model, we aimed to study the role of memory CD8$^+$ T cell recall responses in prevention of persistent infection. For this purpose, we used the sPD1-p24$_{fc}$/EP DNA vaccine [29]. This vaccine exploits the binding of PD-1 to ligands expressed on DCs by fusing soluble PD-1 with HIV-1 GAG p24 antigen. In previous studies, this vaccine consistently elicited up to 21.2% of p24 tetramer-positive CD8$^+$ T cells in the spleen, with broad reactivity, polyfunctionality and cytotoxicity [29]. We also included a non-DC-targeting vaccine, p24$_{fc}$/EP, as a control. Using the same immunization schedule from that work, we immunized groups of BALB/c mice ($n = 5$) with 100 μg DNA intramuscularly via electroporation (EP) three times at 3-week intervals (Fig. 2a). T cell responses to vaccination were measured at 2 weeks after the final vaccination. Subsequently, mice were challenged
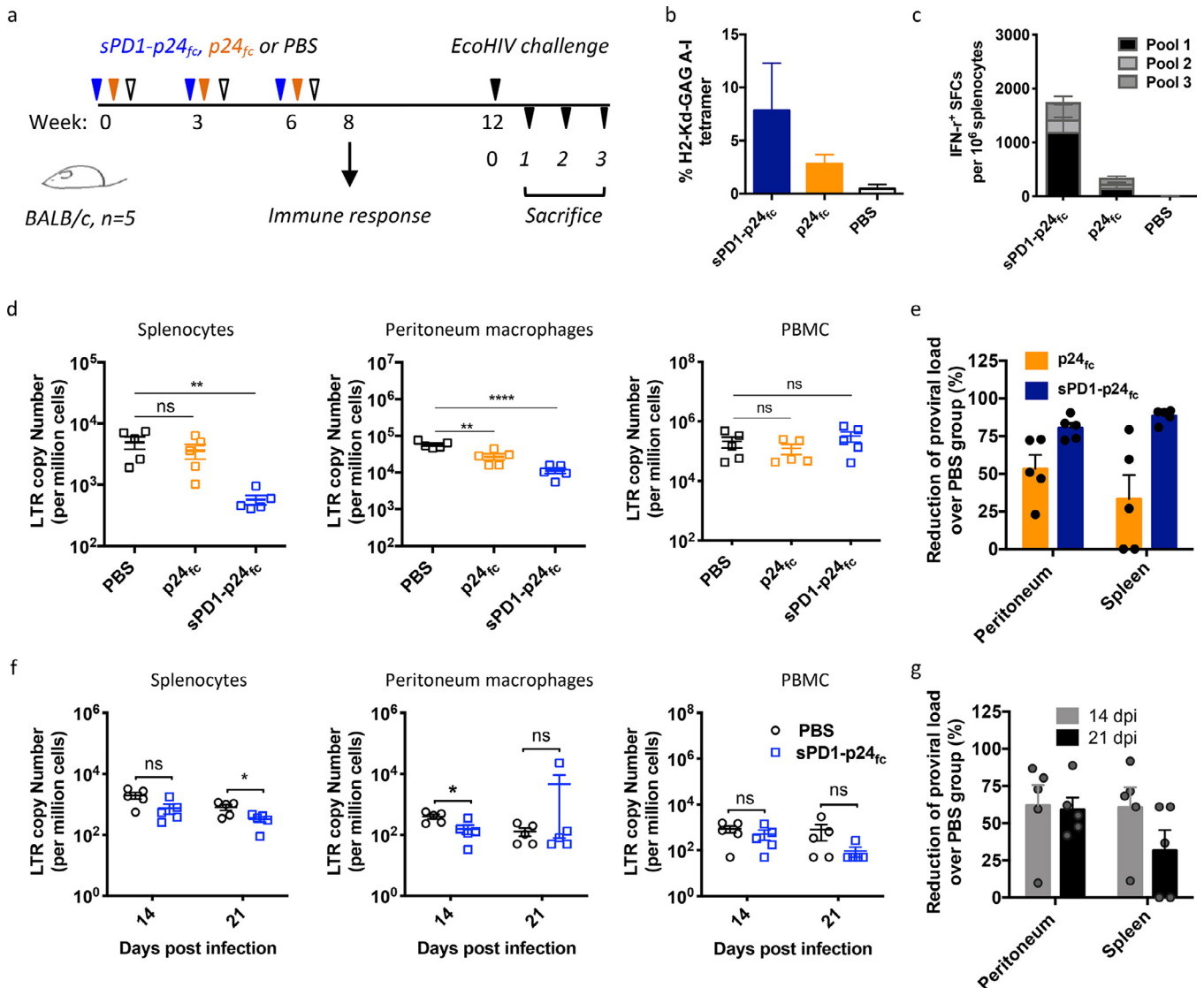

Fig. 2. Prophylactic vaccination-mediated virus clearance was restrained by day 7. a. Experimental design used to investigate the efficacy of sPD1-p24fc/EP DNA in preventing EcoHIV infection. Groups of BALB/c mice ($n = 15$ in each group) were vaccinated with 100 μg sPD1-p24fc/EP or p24fc/EP DNA, or with PBS as a control, intramuscularly at weeks 0, 3, and 6, followed by intraperitoneal challenge with EcoHIV (400 ng p24) 6 weeks after the third vaccination. Five animals from each group were sacrificed at 1, 2 and 3 weeks post-infection (wpi). b. HIV-1 p24-specific H2-Kd-GAG A-I-PE tetramer staining of CD8$^+$ T cell populations two weeks after final immunization and before EcoHIV challenge. c. HIV-1 p24-specific T cell ELISpot responses were determined using three non-overlapping peptide pools. d. Proviral load in the spleen, peritoneal macrophages, and blood were evaluated by examining HIV LTR copy number per million cells by qPCR at 7 dp.i. e. Reduction of proviral loads in the peritoneal macrophages (peritoneum) and spleen for vaccinated mice presented as percentage compared to unimmunized mice data at 7 dp.i. f. Proviral load in the spleen, peritoneal macrophages, and blood based on HIV LTR copy number per million cells as determined by qPCR at 14 and 21 dp.i. g. Reduction of proviral loads in the peritoneal macrophages (peritoneum) and spleen for vaccinated mice presented as percentage compared to unimmunized mice data at 14 and 21 dp.i. Data represent two independent experiments with three (b and c) or five mice (d, e, f, g) per group and with error bars representing the SEM. *, $P < 0.05$; **, $P < 0.01$; ****, $P < 0.0001$. A two-tailed Student t-test and Bonferroni-Holms method was used.

i.p. with EcoHIV (400 ng p24/mouse) 6 weeks after the last vaccination. Proviral load were measured at 7, 14 and 21 dpi. We found that for all groups of mice, levels of H2-Kd-GAG A-I tetramer$^+$ CD8$^+$ T cells in the blood correlated with the potency of the functional CD8$^+$ T cell response elicited by the vaccine [18, 29]. sPD1-p24$_{fc}$/EP vaccination consistently elicited a strong antigen-specific CD8$^+$ T cell response. Up to 19.7% of CD8$^+$ T cells in blood were positive for H2-Kd-GAG A-I tetramer at 2 wpi (Fig. 2b). Three non-overlapping peptide pools spanning the entire p24 protein were also used to stimulate splenocytes of three sacrificed mice from each group, and 200−1000 ELISpots per 10^6 splenocytes were detected with each of these pools in sPD1-p24$_{fc}$-vaccinated mice (Fig. 2c), indicating substantial breadth of the elicited T cell response. In contrast, considerably fewer than 200 ELISpots per 10^6 splenocytes were detected with each of these pools in the control vaccine group (Fig. 2c).

After the EcoHIV challenge, proviruses were readily detected in spleen, peritoneal macrophages and PBMC in all mice (Fig. 2d). In p24$_{fc}$-vaccinated mice, we observed a significant reduction of proviral load in peritoneal macrophages at 7 dpi relative to controls, but not in splenocytes or PBMCs (Fig, 2d). In contrast, there was ~80% reduction of infected cells in the spleen and peritoneal macrophages of sPD1-p24$_{fc}$-vaccinated mice relative to controls at 7 dpi, demonstrating the efficacy of sPD1-p24$_{fc}$/EP in eliminating infected cells (Fig. 2d and 2e). However, we saw no significant reduction in infected cells in peripheral blood. Moreover, we were still able to detect a proviral load in the weeks that followed, suggesting that vaccine-induced CD8$^+$ T cells failed to prevent the establishment of persistent infection (Fig. 2f). It is critical to note that we observed less reduction of proviral load in spleens and peritoneal macrophages from sPD1-p24$_{fc}$-vaccinated mice relative to controls at 14 and 21 dpi (Fig. 2f and 2g), suggesting that accelerated elimination of infected cells by vaccine-induced immunity was abrogated after 7 dpi.

3.3. EcoHIV subverted virus-specific T cell immunity by day 7

To better understand this abrogation, we performed a longitudinal analysis of T cell responses. Virus-specific CD8$^+$ T cells were measured by H2-Kd-GAG A-I tetramer staining of splenocytes at 7, 14 and 21 dpi [18, 29]. We found that high levels of CD8$^+$ T cells were elicited in the spleens of vaccinated mice after viral challenge, with 18.2−41.6% of CD8$^+$ T cells positive for H2-Kd-GAG A-I tetramer at 7 dpi (Fig. 3a). In contrast, we observed less than 1% H2-Kd-GAG A-I tetramer$^+$ CD8$^+$ T cells in control mice, suggesting that infection induces rapid expansion of vaccine-induced virus-specific CD8$^+$ T cells (Fig. S2). However, despite ongoing viral replication, we found a significant decline in virus-specific CD8$^+$ T cells in the spleens of vaccinated mice at 2 and 3 wpi, coinciding with impaired viral clearance. ~4.53−21.20% and 4.01−8.99% of CD8$^+$ T cells in the spleens of vaccinated mice were positive for H2-Kd-GAG A-I tetramer at 14 and 21 dpi, respectively (Fig. 3a and Fig. S2), suggesting rapid suppression of the virus-specific CD8$^+$ T cell response after 7 dpi.

During chronic infection, virus-specific CD8$^+$ T cells persist in a nonfunctional exhausted state and become unresponsive to viral antigens (1). These exhausted CD8$^+$ T cells are characterized by the expression of PD-1 and Tim3 and an inability to proliferate (1). To understand the functional states of virus-specific T cells in EcoHIV-infected mice, we analyzed PD-1 and Tim3 expression, as well as the proliferative capacity of CD4$^+$ and CD8$^+$ T cells in response to ex vivo antigen stimulation. We observed significantly elevated PD-1 and Tim3 expression on CD4$^+$ and CD8$^+$ T cells in the spleens of vaccinated mice at 2 and 3 wpi (Fig. 3b). Significantly increased PD-1 expression was also observed on T cells that are critical for long-lasting protection against virus, CD8$^+$ effector memory (Tem) and CD8$^+$ central memory T cells (Tcm) (Fig. 3c and Fig. S2). We next assessed the proliferative capacity of the T cells. P24 peptide pools that gave a positive cell-mediated immune response by ELISpot were used to stimulate splenocytes in an ex vivo cytofluorimetric proliferation assay based on CFSE staining [29]. To validate this assay and set a threshold for a positive response, we analyzed splenocytes from vaccinated and unchallenged mice stimulated with p24 peptide pools or anti-CD3/CD28 antibodies. We found that T cells from all tested mice showed proliferative responses to CD3/CD28 stimulation. However, only T cells from vaccinated and unchallenged mice proliferated effectively in response to the p24 peptide pools, whereas CD4$^+$ and CD8$^+$ T cells from challenged mice failed to demonstrate proliferation response to p24 peptide (Fig. 3d and 3e). We observed more than 80% inhibition of antigen-specific CD4$^+$ and CD8$^+$ T cell proliferation at 7 dpi, demonstrating the unresponsiveness of those T cells upon viral antigen re-encounter within the first week (Fig. 3f). Moreover, we observed increased levels of Treg cells in spleens of vaccinated mice at 2 and 3 wpi (Fig. 3g). These results suggest that despite an initially efficient T cell recall response, virus-specific T cells become unresponsive to viral antigens and nonfunctional within 7 days after viral challenge, with a notable increase in Treg cell production.

3.4. Therapeutic vaccination fails to accelerate elimination of infected cells

In tumor-bearing mice, repeated sPD1-p24$_{fc}$/EP DNA vaccination produces an active immune state that prevents the emergence of exhausted PD-1$^+$ and Tim-3$^+$ CD8$^+$ T cells and Treg cells, leading to therapeutic cure of pre-existing mesothelioma [18]. We hypothesized that a similar repeated vaccination regimen of sPD1-p24$_{fc}$/EP DNA could boost virus-specific memory CD8$^+$ T cell response in mice and induce further clearance of infected cells. To test this hypothesis, 20 BALB/c mice were immunized intramuscularly three times: 10 animals with msPD1-p24$_{fc}$/EP DNA, and 10 with PBS as a control (Fig. 4a). The sPD1-p24$_{fc}$ DNA vaccine induced a strong virus-specific CD8$^+$ T cell response, with H2-Kd-GAG A-I tetramer$^+$ CD8$^+$ T cells representing 5−14% of PBMCs (Fig. 4b). Subsequently, all 20 animals were challenged i.p. with EcoHIV at a dose of 400 ng p24 at 6 weeks after the last vaccination; five mice in each group (vaccine or PBS) were subsequently immunized intramuscularly with 100 μg sPD1-p24$_{fc}$/EP DNA three times at 3-week intervals, starting at 1 dpi. We sacrificed all mice at 12 wpi, with the exception of one control mouse and two prophylactically vaccinated mice that died before week 12. Vaccine efficacy was investigated by measuring the extent of EcoHIV infection in splenocytes and peritoneal macrophages by qPCR. Virus-specific T cell response was determined by H2-Kd-GAG A-I tetramer staining of splenocytes at week 12. Consistent with previous results, prophylactic vaccination significantly lowered proviral load in both spleen and peritoneal macrophages (Fig. 4c). The proportion of H2-Kd-GAG A-I tetramer$^+$ CD8$^+$ T cells was significantly higher in mice that received both prophylactic and therapeutic vaccination than mice that received prophylactic vaccination alone, suggesting that therapeutic vaccination boosted virus-specific CD8$^+$ T cell reactivation (Fig. 4d). However, we saw no further reduction of proviral load in splenocytes or peritoneal macrophages in these mice (Fig. 4c), indicating that these T cells very likely become exhausted soon after reactivation, similar to the fate of reactivated virus-specific T cells following viral challenge in the prophylactic vaccine group (Fig. 3). We consistently observed high expression of Tim3 and PD-1 in CD8$^+$ T cells in the spleens of both prophylactic-only and prophylactic plus therapeutically vaccinated mice (Fig. 4e). Increased frequency of Treg and MDSC was observed in all challenged mice (Fig. 4f and 4g). Moreover, repeated therapeutic vaccination elicited only low levels of p24-specific CD8$^+$ T cell response in unvaccinated and challenged mice: only 1.87−3.08% of CD8$^+$ T cells in their spleens were H2-Kd-GAG A-I tetramer$^+$ after the third vaccination (Fig. 4d). We conclude that therapeutic vaccination can enhance virus-specific T cell reactivation during early infection, but cannot prevent the rise of exhausted PD-1$^+$ and Tim-3$^+$ CD8$^+$ T or Treg cells, preventing effective cure of EcoHIV infection.
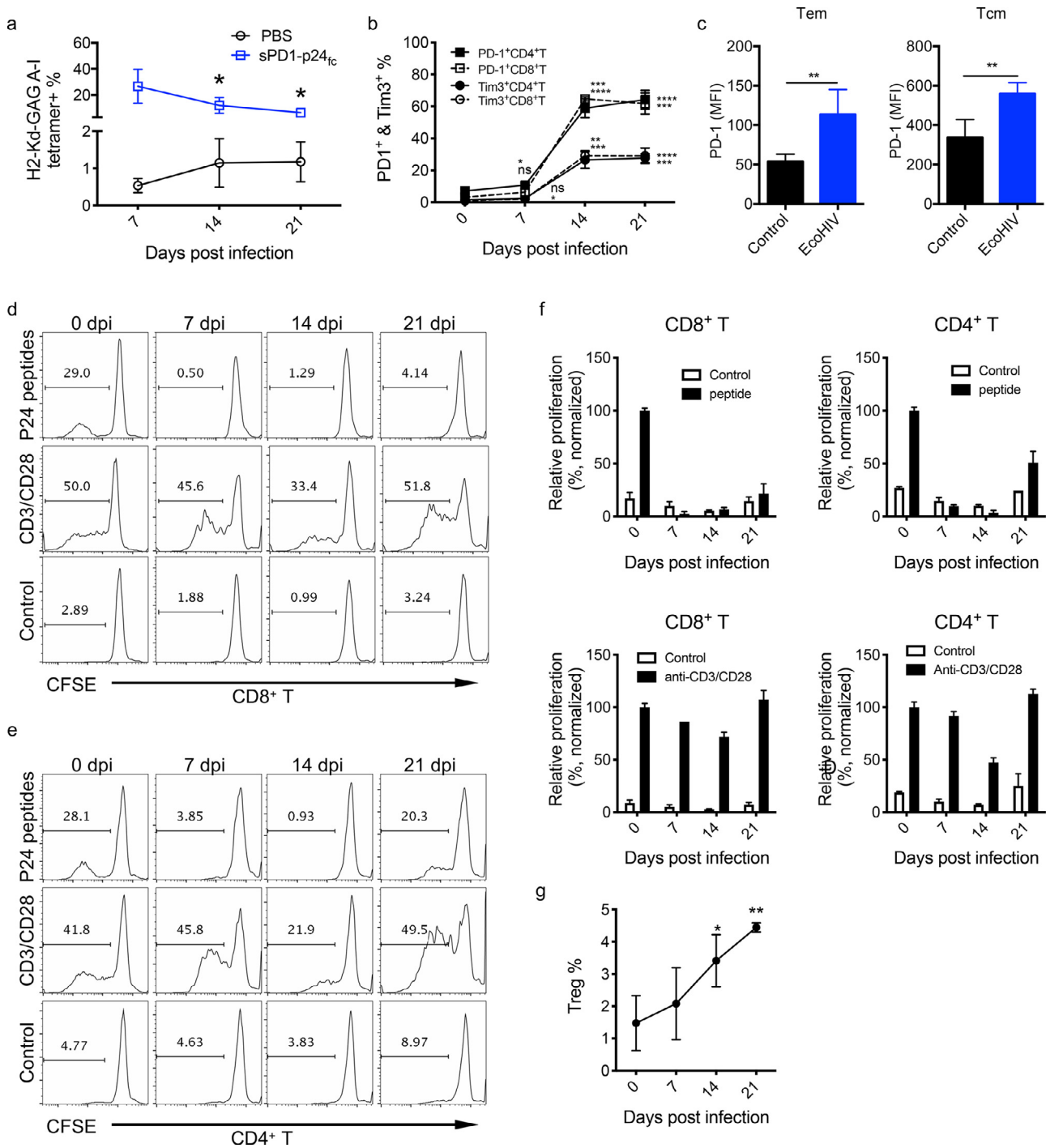
Fig. 3. EcoHIV subverted virus-specific T cell immunity during acute infection. a. HIV-1 p24-specific H2-Kd-GAG A-I-PE tetramer staining of CD8$^+$ T cell populations at 1, 2 and 3 wpi for vaccinated versus unvaccinated mice. b. Increasing numbers of CD4$^+$ and CD8$^+$ T cells express Tim-3 or PD-1 after EcoHIV challenge in BALB/c mice ($n = 5$). Two independent experiments were performed. c. Increased expression level of PD1 on CD8$^+$ Tem and Tcm in spleens at 2 wpi. d, e. Proliferation of (d) CD8$^+$ and (e) CD4$^+$ T cell subsets. Splenocytes were labeled with CFSE and stimulated with p24 peptide pools or anti-CD3 and anti-CD28 antibodies for 5 days. Unstimulated cells were included as controls. CFSE signals were detected by flow cytometry. f. Relative proliferation of CD4$^+$ and CD8$^+$ T cell subsets after peptide (top) or anti-CD3 (bottom) treatment. Data from three separate experiments were normalized relative to data from splenocytes of vaccinated but non-virus-challenged mice, and are shown as mean ± SEM. g. Increased frequencies of CD4$^+$ Treg cells in the spleens during the three weeks post-infection. Data represent mean ± SEM. *, $P < 0.05$; **, $P < 0.01$; ***, $P < 0.001$; ****, $P < 0.0001$. A two-tailed Student t-test and Bonferroni-Holms method was used.

3.5. DCs are activated in ecohiv-infected mice and primed CD8$^+$ T cell ex vivo

DCs play a critical role in CD8$^+$T cell priming and reactivation in vivo [12,13]. To understand the cause of CD8$^+$ T cell non-responsiveness to the therapeutic vaccine and decreased CD8$^+$ T cell number and function during EcoHIV infection, we performed a kinetic analysis of various subpopulations of DCs over 3 weeks after i.p. inoculation of EcoHIV at a dose of 400 ng p24. By flow cytometry, we identified multiple DC populations (Fig. S3), including the two major murine splenic conventional DC (cDC) populations, CD8$^-$ and CD8$^+$; monocyte-derived DCs (Mo-DCs) that are recruited from blood monocytes into lymphatic tissues during infection; and plasmacytoid DCs (pDCs). These cDCs were identified from total non-lymphocytes
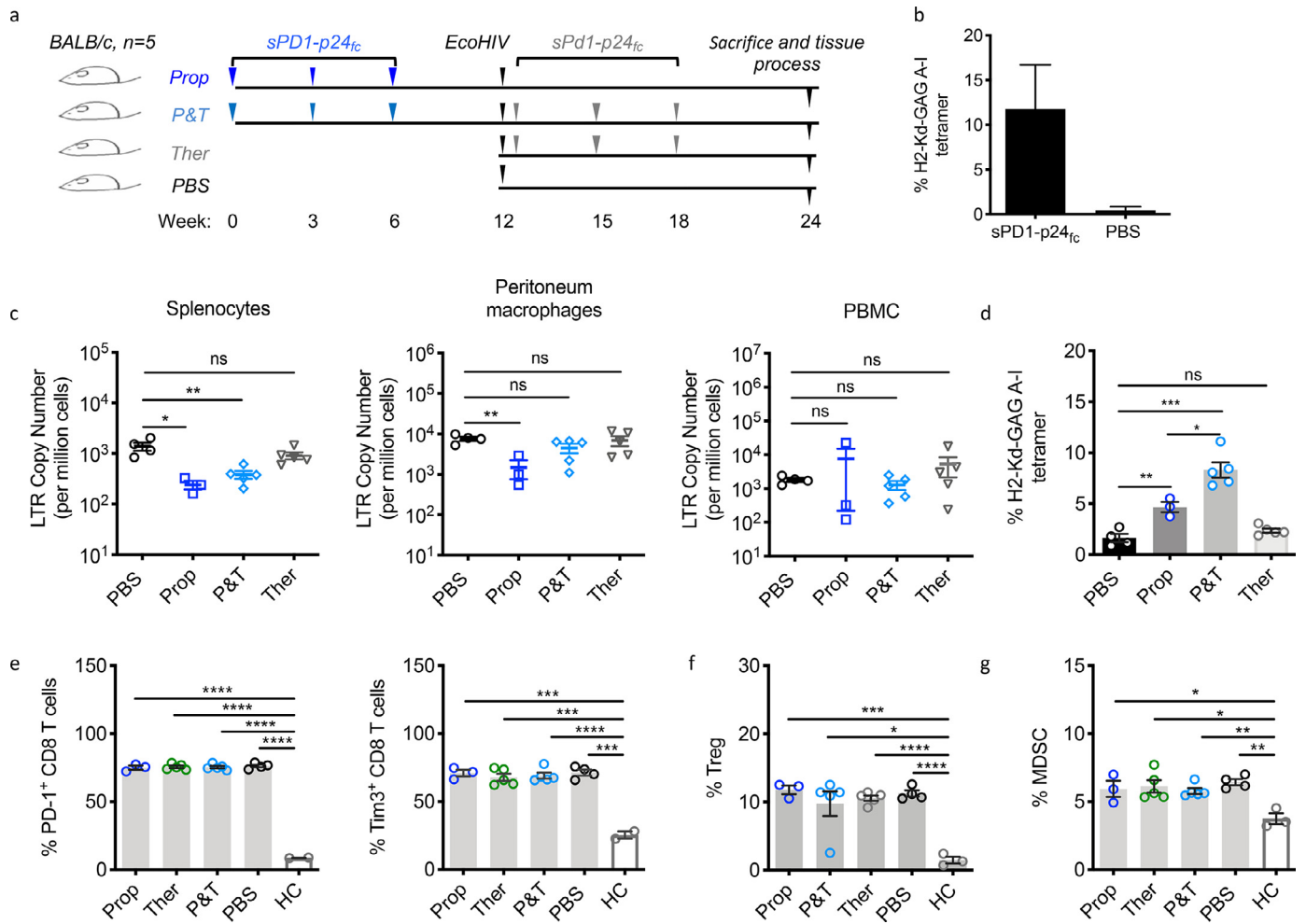
Fig. 4. Therapeutic vaccination failed to accelerate elimination of virus infected cells. a. Experimental design used to investigate the efficacy of sPD1-p24fc/EP DNA vaccine in boosting memory CD8$^+$ T cell reactivation and curing of EcoHIV infection. Two groups (n = 10 per group) of BALB/c mice were subjected to vaccination with DNA (Prop group) or PBS intramuscularly at weeks 0, 3 and 6, followed by intraperitoneal challenge with EcoHIV (400 ng p24) 6 weeks after the third immunization. Five animals from each group were subsequently subjected to DNA vaccination intramuscularly at 2 dpi and 3 and 6 wpi (Ther and P&T groups). All animals were sacrificed at 12 wpi. b. HIV-1 p24-specific H2-Kd-GAG A-I-PE tetramer staining of CD8$^+$ T cell populations 2 weeks after the final immunization. c. Proviral load in the spleen, peritoneal macrophages and blood were evaluated by examining HIV LTR copy number per million cells by qPCR. d. HIV-1 p24-specific H2-Kd-GAG A-I-PE tetramer staining of CD8$^+$ T cell populations at 12 wpi for all four groups of mice. e-g. Assessment of CD4$^+$ and CD8$^+$ T cells after viral challenge in BALB/c mice (n = 5) for (e) the expression of PD-1 (left) or Tim-3 (right), and frequencies of (f) CD4$^+$ Treg and (g) MDSCs. Data represent mean ± SEM of two independent experiments with 3−5 mice per group. *, $P < 0.05$; **, $P < 0.01$; ***, $P < 0.001$; ****, $P < 0.0001$. A two-tailed Student t-test and Bonferroni-Holms method was used.

by high expression of CD11c and lack of Ly6C. Mo-DCs were identified by high expression of CD11c, CD11b, and Ly6C. pDCs can be identified based on CD11c^{lo}, B220$^+$, Ly6C$^+$, and CD11b$^-$. CD8$^+$ DCs and Mo-DCs cross-present antigens phagocytosed from the environment via MHC class I, and are potent initiators of CD8$^+$ T cell responses, whereas CD8$^-$ DCs primarily initiate a Th2 cell response [37,38]. pDCs are the most potent type I interferon (IFN-I)-producing cells in response to viral infection in humans and mice, and provide critical resistance to infection by limiting viral spread and by activating multiple innate and adaptive immune cells [39].

We found that the overall proportion of DCs increased in the spleen over the course of three weeks of infection, whilst CD4$^+$ and CD8$^+$ T cells progressively decreased (Fig. 5a). Among the various DC populations, the proportion of CD8$^+$ cDCs and Mo-DCs increased by about 50% during the first week of infection, but subsequently decreased over the following weeks (Fig. 5b). CD8$^-$ DCs continually increased over the 3-week period, nearly doubling in number between week 1 and 2 (Fig. 5b). We then gauged DC activation based on expression of costimulatory and inhibitory markers. We found that all four DC subsets showed elevated expression of costimulatory receptors CD80 and CD86, as well as the inhibitory receptors PD-L1

and PD-L2, compared to unchallenged mice (Fig. S4). These results suggest expansion and activation of these DC subsets by EcoHIV. We therefore conducted a longitudinal analysis of the stimulatory capacity of DCs from EcoHIV-infected spleens. CD11c$^+$ DCs isolated at 1, 2, 3, 5, 7, 14, or 21 dpi were cultured with ovalbumin (OVA)-specific CD8$^+$ cells from OT-I mice, those with transgenic inserts for mouse Tcra-V2 and Tcrb-V5 genes designed to recognize ovalbumin residues, and the OVA-SIINFEKL peptide for 5 days. Our *ex vivo* data showed that EcoHIV infection resulted in increased DC stimulatory capacity at day 1, and these DCs remained functional in priming CD8 T cells ex vivo during the following weeks (Fig. 5c and 5d).

3.6. EcoHIV induces rapid expansion of MDSCs that inhibited T cells proliferation

MDSCs have emerged as a major suppressor of immune response in chronic infection and cancer [18,19,24]. To understand the rapidly suppressed T cell response in EcoHIV-infected mice, we evaluated myeloid cell populations over three weeks of infection. The proportion of MDSCs, identified as Gr1$^+$ and CD11b$^+$ in Figure S3, increased at day 7, reaching about 2-fold expansion relative to uninfected mice
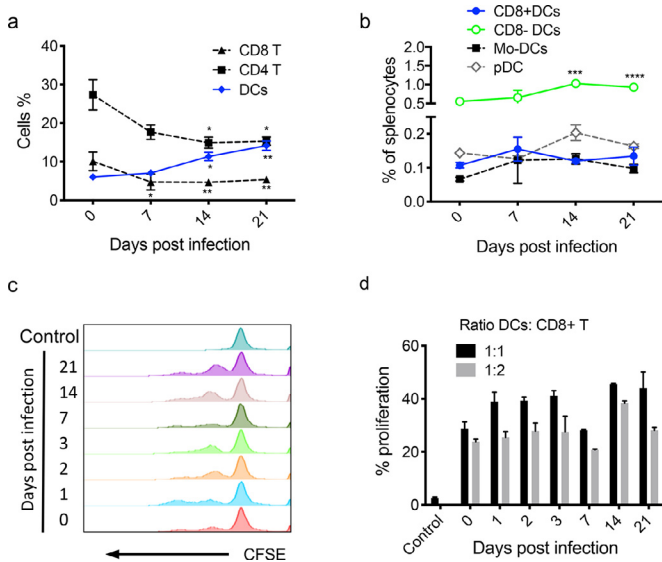
Fig. 5. DCs in EcoHIV-infected mice remain functional in priming CD8$^+$ T cells. a. Changes in the percentages of DCs and T cells in the spleens during the three weeks post-infection. b. DC subpopulations in the spleen were quantified during the three weeks of EcoHIV infection (n = 3) by flow cytometry analysis. Data are representative of two experiments with error bars representing the SEM. c, d. DCs in EcoHIV-infected mice remained functional in priming CD8$^+$ T cells. CFSE-labeled OT-I T cells were cultured with CD11c$^+$ DCs isolated over 3 weeks post-infection. Cultures were stimulated with an OVA peptide SIINFEKL or no peptide as control. Proliferation was measured by flow cytometry after 5 days of culture. Data represent three independent experiments with five mice per group, and is shown in a histogram of one representative experiment (c) or in data represented as a column graph with error bars representing the SEM (d). *, $P < 0.05$; **, $P < 0.01$; ***, $P < 0.001$; ****, $P<0.0001$. A two-tailed Student t-test and Bonferroni-Holms method was used.
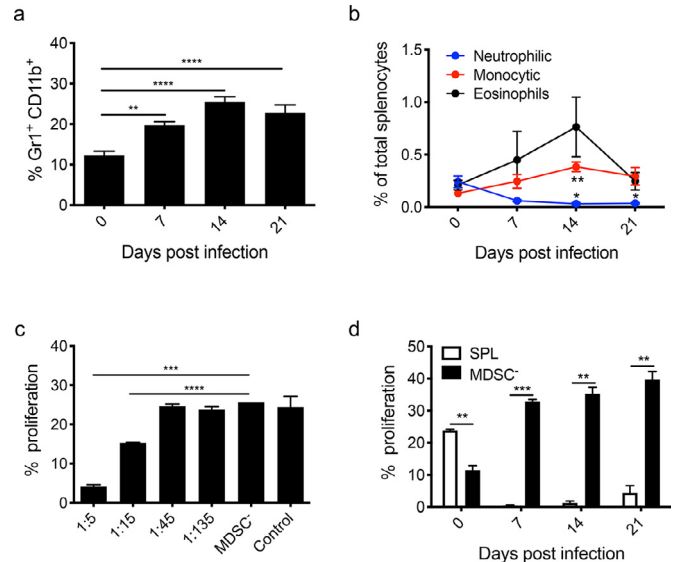
Fig. 6. EcoHIV induces sustained MDSC expansion that inhibits T cell proliferation. a, b. Increased percentage of spleen MDSCs (a) and individual myeloid cell subpopulations (b) were determined by flow cytometry analysis during the 3 weeks post-infection in immunized mice (n = 3). c. MDSCs from EcoHIV-infected mice suppressed CD8$^+$ T cell proliferation in a number-dependent fashion. Splenocytes from sPD1-p24fc/EP DNA-vaccinated but unchallenged mice were cultured with Gr1$^+$ cells from 14 dpi at the indicated ratios and then stimulated with p24 peptide pools. Same number of splenocytes from sPD1-p24fc/EP DNA-vaccinated but unchallenged mice were cultured without Gr1+ cells or with Gr1+ cells from naïve mice in a 1:5 ratio were used as controls. Proliferation was determined by CFSE signals from CD8$^+$ T cell populations based on flow cytometry. Data is shown in a column graph as mean ± SEM. d. Proliferative response of CD8$^+$ T cells to p24 peptides was rescued after depletion of MDSCs. Total splenocytes (SPL) and MDSC-depleted splenocytes (MDSC$^-$) from vaccinated and Eco-HIV-infected mice (n = 3) were labeled with CFSE and stimulated with p24 peptide pools for 5 days. MDSC-depleted splenocytes from vaccinated and unchallenged mice (n = 3) were included as controls. CFSE signals from CD8$^+$ T cell populations were detected by flow cytometry. Data is shown in a column graph as mean ± SEM. Data represent three independent experiments with five mice per group. *, $P < 0.05$; **, $P < 0.01$; ***, $P < 0.001$; ****, $P<0.0001$. A two-tailed Student t-test and Bonferroni-Holms method was used.

(Fig. 6a). These cells continued to increase, peaking at day 14 with nearly 3-fold more MDSCs than in naïve mice. We then determined the cellular composition of this population. Total MDSCs were subdivided into three main populations: Gr1^{lo}Ly6C^{lo}F4/80$^+$SSC^{hi} eosinophils, Gr1^{lo}Ly6C^{hi}F4/80$^+$SSC^{lo} monocytic cells, and Gr1^{hi}Ly6C^{int}F4/80$^-$SSC^{int} neutrophilic cells (Fig. S4) [24]. The number of neutrophilic cells substantially decreased during the first two weeks of infection by about 10-fold before rebounding by week 3 (Fig. 6b). Both monocytes and eosinophils expanded during the first two weeks of infection, peaking at day 14. Eosinophils subsequently contracted to naïve levels by day 21, while monocyte numbers remained high: nearly three-fold higher than naïve mice at day 21. All three populations showed increased expression of inhibitory receptors PD-L1 and PD-L2 after day 14 (Fig. S5a).

The increase in MDSCs during EcoHIV infection coincided with the functional exhaustion of virus-specific CD8$^+$ T cells (Fig. 3 and 6a), raising the possibility that MDSCs suppress the EcoHIV-specific CD8$^+$ T cell response. To assess whether these cells were immunosuppressive, we co-cultured Gr1$^+$ MDSCs isolated from EcoHIV-infected mice with total splenocytes from vaccinated but unchallenged mice at different ratios ranging from 1:5 to 1:135, and stimulated them with p24 peptide pools. Gr1$^+$ MDSCs from naive mice were tested as a control. We found that Gr1$^+$ MDSCs from EcoHIV-infected mice suppressed CD8$^+$ T cell proliferation in a cell number-dependent manner (Fig. 6c and Fig. S5b). Naïve control Gr1$^+$ cells had no effect on T cell proliferation, even at 1:5 ratio (Fig. SS5b). To further confirm that MDSCs inhibit CD8$^+$ T cell proliferation, we used an anti-Gr1 antibody to deplete total MDSCs from splenocyte populations collected from vaccinated and EcoHIV-challenged mice. After 7 days culture with p24 peptide pools, the proliferative response of CD8$^+$ T cells to p24 peptides was fully rescued in MDSC-depleted cultures (Fig. 6d), in strong contrast to the non-responsiveness of CD8$^+$ T cells cultured with total splenocytes. Therefore, we conclude that EcoHIV induces

rapid expansion of MDSCs that inhibit CD8$^+$ T cell proliferation within the first week of infection.

3.7. MDSCs are infected and resistant to CD8$^+$ T cell-induced apoptosis

To characterize the infected cells that escape from vaccine-induced CTL killing, we measured the phenotype of p24$^+$ cells in the spleen at 2 and 3 wpi by flow cytometry. Besides a small population of p24$^+$ CD4$^+$ T cells, by 2 wpi more than 80% of p24$^+$cells in the spleens were CD11b$^+$Gr1$^+$ MDSCs (Fig. S6a). At week 3, there was a significant decline of p24$^+$CD4$^+$ T cells in the spleen, but not p24$^+$Gr1$^+$ cells (Fig. 7a). We then determined the cellular composition of p24$^+$MDSCs by subdividing the MDSCs into monocytes, neutrophils, and eosinophils (as defined above) over the course of three weeks. We found that both p24$^+$monocytic and neutrophilic cell populations expanded during the first two weeks of infection (Fig. 7b and Fig. S6b). Expansion of neutrophilic cells peaked at day 14 and remained high at day 21, while monocytic cells continued to increase at day 21, reaching ~3-fold expansion relative to day 14 (Fig. 7b), suggesting enrichment of EcoHIV-infected monocytic cells. Consistently with this hypothesis, IHC staining showed that almost all p24$^+$ cells in the spleen were Gr1$^+$ at 12 wpi (Fig. 7c), suggesting that infected MDSCs likely represent a cell type that escapes host immunity.

We have previously reported that sPD1-p24$_{fc}$ elicited functional antigen-specific CD8$^+$ T cells can eliminate MDSCs through apoptosis in a malignant mesothelioma mouse model [18,40]. We therefore compared the interaction between vaccine-induced CD8$^+$ T cells and
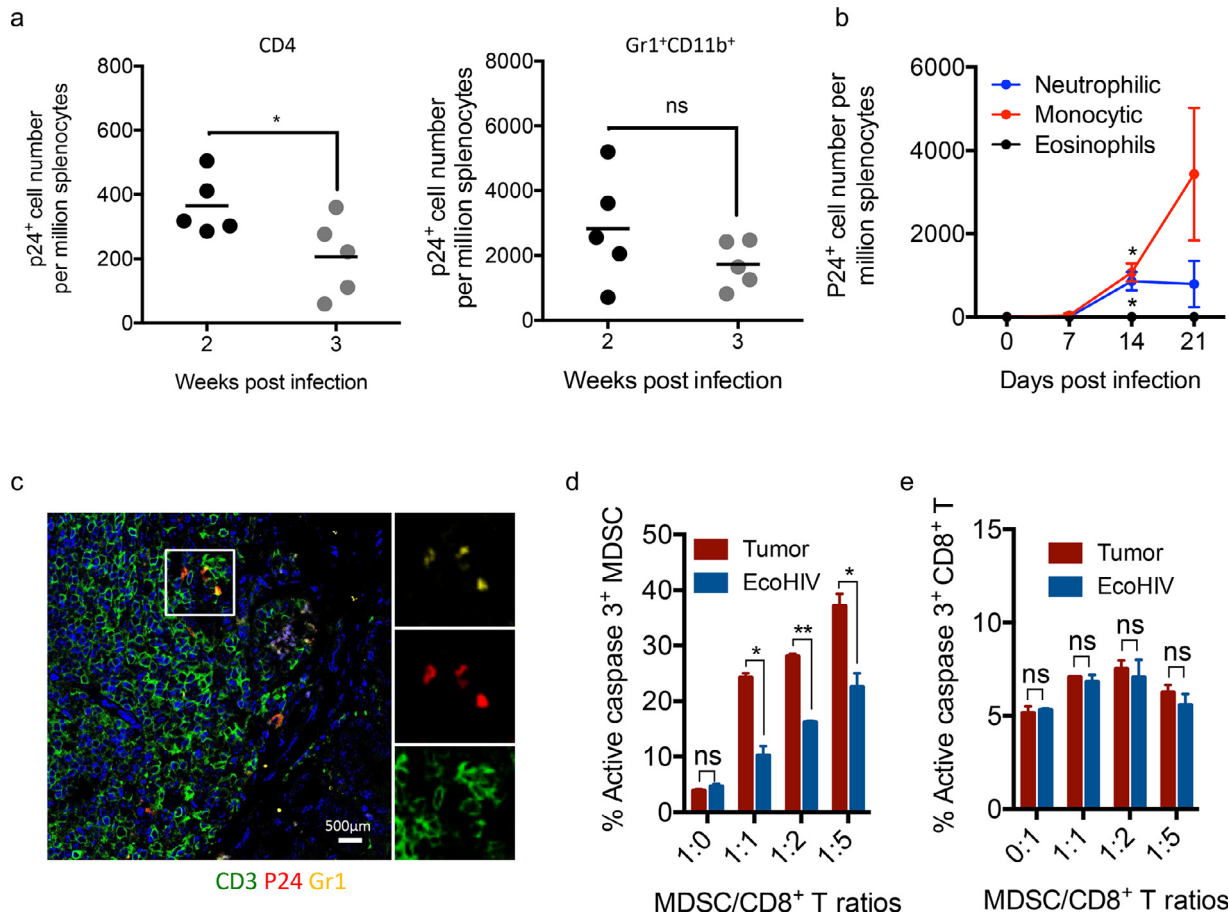
Fig. 7. Myeloid cells are infected and resistant to CD8+ T cells-induced apoptosis. a. p24$^+$ spleen cells were analyzed at 2 and 3 wpi by flow cytometry. Counts are shown from two experiments (n = 5), with mean ± SEM. P24$^+$ cells included CD4$^+$ T cells and MDSCs (Gr1$^+$CD11b$^+$). *P < 0.05. b. p24$^+$ spleen myeloid cell subpopulations during the 3 weeks post-infection (n = 3) were analyzed by flow cytometry and are shown as mean ± SEM. Uninfected mice stained with anti-p24 antibody served as control. c. Staining of EcoHIV-infected spleen using antibodies against p24 protein (TRITC; red), CD3 (FITC; green), Gr1 (Alexa-647, yellow), and DAPI (Blue) at 12 wpi. d. Apoptosis of MDSCs from malignant mesothelioma and EcoHIV-infected mice was measured based on expression of caspase-3 after co-culturing with CD8$^+$ T cells from vaccinated mice for 24 hrs. Data is shown in a column graph as mean ± SEM. e. MDSCs do not induce significant apoptosis of CD8$^+$ T cells, with data shown as in a column graph as mean ± SEM. Data represent three independent experiments with five mice per group. *, P < 0.05; **, P < 0.01; ***, P < 0.001; ****, P<0.0001. A two-tailed Student t-test and Bonferroni-Holms method was used.

MDSCs derived either from EcoHIV-infected mice at day 14 or MDSCs from the malignant mesothelioma model. Virus-specific CD8$^+$ T cells from vaccinated and unchallenged mice were co-cultured with MDSCs from either EcoHIV-infected mice or malignant mesothelioma mice for analysis of active caspase-3 via flow cytometry as described previously [18, 40]. Consistent with previous findings, virus-specific CD8$^+$ T cells caused apoptosis in MDSCs from both mouse models in a cell number-dependent manner (Fig. 7d). However, compared with MDSCs from the cancer model, GAG-specific CD8$^+$ T cells caused significantly less apoptosis of co-cultured MDSCs from EcoHIV-infected mice (Fig. 7d). In the same experiment, the coculture did not result in significant levels of apoptosis in CD8$^+$ T cells (Fig. 7e). These data provide evidence that MDSCs from EcoHIV-infected mice are relatively resistant to CTL-mediated apoptosis, which might contribute to viral evasion from vaccine protection.

3.8. Antibody depletion of mdsc enhances clearance of eohiv-infected cells in vivo

To test whether depletion of MDSCs will enhance clearance of EcoHIV-infected cells in vivo through direct depletion of infected myeloid cells and boost of T cell function, we monitored the abundance of Gr1$^+$ cells in the blood of three naïve mice for 5 days after a single injection of 100 ug anti-Gr1 as previously described [24] (Fig. S7). Treatment with anti-Gr1 significantly reduced the

abundance of Gr1$^+$ myeloid cells to less than 1% in the blood after 1 day, and there was no significant increase in Gr1$^+$ cells in the blood after 5 days of treatment (Fig. S7a and 7b). It was previously reported that anti-Gr1 does not completely deplete Gr1$^+$ cells. A small population with the antibody on the surface will remain for more than 4 days, and will not be detected by fluorophore-conjugated RB6−8C5 (Ly6C/G) and 1A8 (anti-Ly6G) antibody staining [24]. Therefore, we measured total blood myeloid cells with an antibody against CD11b. We found that treatment with anti-Gr1 reduced total myeloid cells by more than 80% after 1 day, from ~35% to < 7%. Abundance of myeloid cells did not increase significantly at day 2 and 3, and by day 5, increased to ~10% in treated mice (Fig. S7a and 7c).

We next immunized groups of BALB/c mice (n = 5) with 100 μg sPD1-p24$_{fc}$ DNA intramuscularly via EP three times at 3-week intervals (Fig. 8a). Subsequently, mice were challenged intraperitoneally with EcoHIV (400 ng p24/mouse) at 6 weeks after the last vaccination. 100 μg of anti-Gr1 or control antibody (rat IgG2b) was given on days 7, 9, and 11. At day 1 after the 1st antibody injection, we found reduction of total CD11b$^+$ and Gr1$^+$ myeloid cells by around 70% and more than 99% in the blood (Fig. 8b). Significant reduction of DCs subpopulations that express Ly6c, Mo-DC and pDC, was also observed (Fig. 8c). At 14 dpi, mice were sacrificed, and frequency of MDSCs and DCs and provirus copies were tested in blood, spleen and peritoneal macrophages from all mice. In the blood, we found significant reduction of MDSC and Mo-DC in depleted mice (Fig. 8d). Moreover,
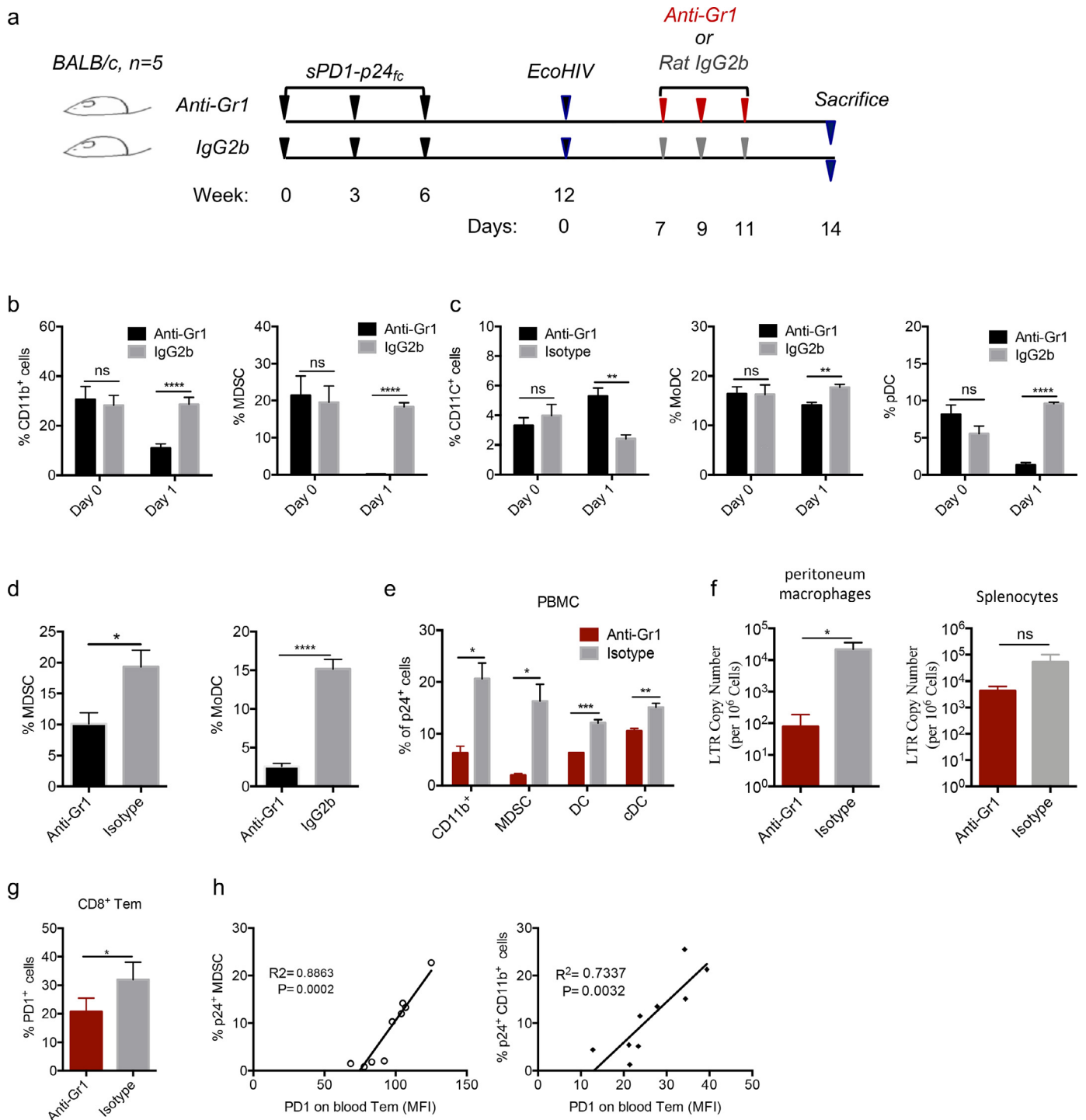
Fig. 8. Antibody depletion of myeloid cells enhances clearance of EcoHIV-infected cells in vivo. a. Experimental schedule. Two groups of BALB/c mice (*n* = 5/group) were vaccinated with 100 μg sPD1-p24fc/EP DNA intramuscularly at weeks 0, 3, and 6, followed by intraperitoneal challenge with EcoHIV (400 ng p24) at 6 weeks after the third vaccination. Mice were then treated with 100 μg of anti-Gr1 or control antibody at 7, 9 and 11 dpi, and sacrificed at 14 dpi. b. The percentage of CD11b⁺ myeloid cells and Gr1⁺ cells in blood at day 1 after anti-Gr1 treatment. c. The percentage of CD11C⁺ total DCs, Mo-DCs and pDCs in blood at day 1 after anti-Gr1 treatment. d. The percentage of MDSCs and Mo-DCs in blood at day 7 after anti-Gr1 treatment. e. The percentage of p24⁺ CD11b⁺ myeloid cells, Gr1⁺ cells CD11C⁺ total DCs, and cDCs in blood at day 7 after anti-Gr1 treatment. f. Proviral load in the peritoneal macrophages and splenocytes were evaluated by examining HIV LTR copy number per million cells by qPCR. g. The percentage of PD1⁺ CD8⁺ Tem in blood at day 7 after anti-Gr1 treatment. Columns represent the mean values of experiment with 5 mice per group, with error bars representing the SEM. Data represent two independent experiments with five mice per group. *, $P < 0.05$; **, $P < 0.01$; ***, $P < 0.001$; ****, $P < 0.0001$. A two-tailed Student *t*-test and Bonferroni-Holms method was used. h. Strong positive correlation between percentage of PD1⁺ CD8⁺ Tem and p24⁺ MDSC (left) and CD11b⁺ myeloid cells in blood at day 7 after anti-Gr1 treatment. Liner regression was used.

depleted mice have lower frequency of p24⁺ blood MDSC, and a ~600-fold reduction of proviral loads in peritoneum macrophages (Fig. 8e and 8f). These results suggest that depletion of MDSC enhanced clearance of EcoHIV infected cells. The number of p24⁺ cDC, a population that do not express ly6c, were also significantly

reduced in the blood of depleted mice (Fig. 8e), suggesting an enhanced clearance of viral infection by host immunity. Further analysis revealed that expression level of PD-1 on CD8⁺ Tem in blood was significantly decreased in these mice (Fig. 8g), suggesting a boost of T cell function. Moreover, statistical analysis showed that expression of

PD1 on blood Tem is positively correlated with frequency of p24$^+$ MDSC and CD11b$^+$ myeloid cells (Fig. 8h). In the spleen, only Mo-DC were significantly reduced in anti-Gr1 treated mice (Fig. S8A). Moreover, depleted mice tended to have an increase in interferon γ-producing p24-specific T cells (Fig. S8b, 8c and 8d), reduced proviral loads in the spleen (Fig. 8f). However, these differences were not statistically significant, suggesting a limited effect of anti-Gr1 antibody on depletion of MDSCs and reduction of EcoHIV infection there. Our data suggest that by reducing the numbers of ly6c$^+$cells, we were able to enhance elimination of infected cells in vivo, and likely boosted CD8$^+$ T cell function to clear infected ly6c negative cells.

4. Discussion

Here we have identified an unexpected role of myeloid cells in facilitating viral evasion of memory CD8$^+$ T cell response at very early stage of viral infection. We present an extensive analysis of innate cell activation and memory CD8$^+$ T cell response following virus challenge of vaccinated, immunocompetent BALB/c mice. Our results indicate that EcoHIV activates DCs and myeloid cells during the first week of infection, and initiates both effective CD8$^+$ T cell priming in naïve mice and recall of memory T cells response and effector function in vaccinated mice. However, myeloid cells serve as shelters to provide a mechanism for the virus to escape CTL-mediated apoptosis, and infection led to rapid expansion and accumulation of myeloid cells with T cell-suppressive function, resulting in diminished virus-specific CD8$^+$ T cell numbers and function, and reduced vaccine-mediated virus clearance within 7 dpi. These data provide not only a detailed picture of DC, myeloid cell, and memory CD8$^+$ T cell reactivation in response to persistent viral infection, but also new insight into the mechanisms that underlie lentiviral evasion of vaccine-induced T cell immunity to establish persistent infection.

Thus far, it has remained unclear when and to what extent persistent infection suppresses CD8$^+$ memory T cell reactivation during recall response. Data are currently only available regarding the role of MDSCs in suppressing CD8$^+$ T cell function during primary infection [20,24,32]. We recently developed a sPD1-p24$_{fc}$/EP DNA DC-targeting vaccine, which induces a strong and durable HIV-1 GAG-specific CD8$^+$ T lymphocyte response, with broad reactivity, polyfunctionality and cytotoxicity [29]. We have now utilized this model vaccine to investigate its potential to confer complete protection against persistent lentiviral infection. We have analyzed the secondary T cell immune response to EcoHIV, a persistent lentivirus that induces immunosuppression during infection, and the role of the recall responses in preventing persistent infection. We found that after EcoHIV challenge, there was robust proliferation of antigen-specific CD8$^+$ T cells, which reduced the number of virus-infected cells in spleen and Peritoneum macrophages before day 7. However, EcoHIV also infected MDSCs, which are resistant to CD8$^+$ T cell-mediated killing, while also inducing a rapid expansion of this cell population (Fig. 6 and Fig. 7). The expanded MDSCs profoundly subverted the memory CD8$^+$ T cell response in terms of both number and function at a very early stage of infection, resulting in persistent viral infection. Our data have revealed the time-course of this process, and the important role of myeloid cells in subverting memory recall responses to virus and thereby facilitating viral persistence. We did not observe significant reduction of proviral load in PBMC in sPD1-p24$_{fc}$ vaccinated and challenged mice, which might be due to the higher frequency of MDSCs in the blood compared to spleen (Fig. 8b and Fig. 1h), and the resistance of infected MDSC to CD8$^+$ T cell-mediated killing.

Our description of the expansion of Gr1$^+$ myeloid cells following EcoHIV challenge in vaccinated mice is similar to the phenomenon observed in chronic LCMV [24,41]. Previous studies using models of acute and chronic LCMV infection, the ARM and C13 strains [42,43], respectively, induced accumulation of Ly6C^{hi} monocytes and Gr1^{hi} neutrophils in lymphoid organs and blood during the first three

days [24]. However, the expansion of myeloid cells was only enhanced and sustained over time after peaking at 14 dpi in persistent C13 virus infection, but not in the ARM strain [24]. In our study, accumulation of MDSCs in vaccinated and EcoHIV-challenged mice started before 7 dpi and likewise peaked at 14 dpi. In C13 infection, both DCs and myeloid cells are capable of stimulating T cell proliferation during the first few days of infection, and CD11b$^+$ myeloid cells only begin actively suppressing the priming of T cells at 14 dpi [44,45]. But in EcoHIV-infected mice, only DCs are functional in T cell priming (Fig. 5). Myeloid cells from EcoHIV-infected mice were not able to stimulate T cell proliferation before 7 dpi (data not shown). Instead, Gr1$^+$ cells suppressed memory CD8$^+$ T cells proliferation during this time period in vaccinated and EcoHIV-challenged mice (Fig. 6), suggesting earlier induction of MDSCs during secondary response. This might be because memory T cells response employ different mechanisms from those involved in the priming of naïve T cells. It is also possible that a robust memory CD8$^+$ T cell response during the first few days of EcoHIV infection accelerated MDSC induction. Consistent with this, it has previously been reported that interferon γ produced by effector T cells upon recognition of viral antigens can induce iNOS production in monocytic cells, which in turn inhibits T cell function [46]. Interestingly, there is a slight recovery of CD4$^+$ T cell proliferation at 3 wpi, coincide with the slightly drop of MDSC frequency (Fig. 3).

Of note, persistent LCMV infection has been linked to increased susceptibility of DCs and myeloid derived cells to infection [47,48]. Their faster replication in DCs and myeloid cells outpaces the ability of the adaptive immune response to contain the infection, while also driving excessive immune activation, and inducing MDSC expansion [43,48]. MDSCs repress T cell function, and consequently hinder viral clearance [46]. Although the frequency of EcoHIV infected cells is lower in mice overall, it also infects DCs and myeloid cells (Fig. 6 and Fig. 8), and induces MDSC expansion. Unlike C13-infected mice, in which the majority of MDSCs are neutrophils, EcoHIV induced ly6c^{hi} monocytic myeloid cell expansion, with continuous reduction of Gr1^{hi} neutrophils. Further investigation revealed that both monocytes and neutrophils are infected. However, MDSCs from EcoHIV-infected mice were more resistant to CTL-mediated apoptosis compared to MDSCs from our malignant mesothelioma model (Fig. 7), in which most MDSCs are Gr1^{hi} MDSCs [18], suggesting that EcoHIV induced monocytes might be more resistant to CTL-mediated apoptosis, while infected neutrophils were eliminated by virus-specific CD8$^+$ T cells.

Similarly, induction of myeloid cells expansion was demonstrated in blood of SIV infected macaques after two weeks of virus inoculation [32]. Expansion of MDSC in blood of HIV patients have also been observed in recent years [49]. However, infection of MDSCs during HIV/SIV infection has not been reported. Moreover, the impact of MDSC on HIV vaccine strategies, in particular on HIV therapeutic vaccine remains unknown. Our data suggests that MDSCs was induced and suppressed T cell recall response as early as 7 dpi in vaccinated and EcoHIV-challenged mice. In EcoHIV-challenged naïve mice, repeated therapeutic vaccination elicited only low levels of p24-specific CD8$^+$ T cell response (Fig. 4d). It is unclear whether EcoHIV infection suppressed CD8$^+$ T cell priming by therapeutic vaccination, or first immunization-primed, antigen-specific CD8$^+$ T cells quickly became exhausted in infected mice. Testing earlier timepoints post vaccination would reveal whether these T cells quickly became exhausted or were never elicited. The role of MDSCs on antiviral T cell memory recall responses in HIV vaccine clinical trial or macaque model of SIV/SHIV infection might be important to investigate for developing effective vaccines.

We depleted myeloid cells during EcoHIV infection using an antibody (RB6−8C5) that recognizes Gr1. Gr1 is a marker predominantly expressed by MDSCs, and has been used in many studies to deplete neutrophils, monocytes, and MDSCs [24,50]. We tested the dose of

antibody delivery that could reduce MDSCs in the blood by > 90% (Fig. S7), and subsequently used the same dose and regimen of antibody to deplete MDSCs in vaccinated and infected mice. We found significant decrease of total myeloid cells, MDSCs and ly6c$^+$ pDCs and Mo-DCs at day 1 after antibody injection. Moreover, the loss of myeloid cells and pDCs correlated with decreased PD1 expression on CD8$^+$ Tem cells, and significantly lowered frequency of p24$^+$ cells and proviral load in peritoneal macrophages (Fig. 8). Surprisingly, we did not observe a significant impact on proviral loads in the spleen. The failure to reduce provirus in spleen significantly may be due to multiple factors. Although myeloid cells are infected by EcoHIV, the frequency of these cells in the spleen is relatively low (Fig. 1), and were not effectively depleted (Fig. S8). Moreover, they are but one of many cell types infected by EcoHIV at 2 wpi, including DCs (Fig. 8) and CD4$^+$ T cells (Fig. 7). We did not observe a significant increase in memory CD8$^+$ T cell response, which is likely because MDSCs are just one of several factors involved in the suppression of T cell responses during chronic infection. Other factors, such as Treg cells, and PD1-PDL1 pathway, IL-10, and TGF-β, might suppress T cell response in MDSCs depleted mice. Moreover, Mo-DCs and pDCs also express ly6c, and were depleted by anti-Gr1 antibody. The depletion of Mo-DCs and pDC might compromise the T cell response in vivo. In summary, we demonstrated that depletion of MDSC can enhance viral clearance in vaccinated mice. We believe that strategies that counteract the effects of MDSCs during acute infection could be highly valuable for the development of effective vaccines against chronic human infections like HIV and other persistent virus.

Funding sources

Author contributions

ZC, HW and LL are the principal investigator and co-principal investigators with overall responsibility for the design of the study. LL, QL and JP analyzed the data. LL, ZC, WH and KY contributed to drafting the manuscript. LL, QL, PJ, ZD and JS extracted plasmid DNA and/or generated virus. LQ, PJ, LL, TZ, HK and TH coordinated the viral inoculation, autopsy organization, and collection of autopsy materials of mice. LL, KN, QL and JL was involved in the development and performance of the q-PCR assay. LL and KH were involved in the development and conduct of the H&E and IHC assays. LL, QL, PJ, TZ, TH, KL and FJ conducted T cell proliferation, ELISpot and FACS analyses. All authors were involved in the interpretation of the data.

Declarations of interests

The authors declare no financial or commercial conflicts of interest.

Acknowledgments

Supplementary materials

Supplementary material associated with this article can be found, in the online version, at doi:10.1016/j.ebiom.2020.103008.

References

[1] Li Q, Skinner PJ, Ha SJ, Duan L, Mattila TL, Hage A, et al. Visualizing antigen-specific and infected cells in situ predicts outcomes in early viral infection. Science 2009;323(5922):1726–9.

[2] Virgin HW, Walker BD. Immunology and the elusive AIDS vaccine. Nature 2010;464(7286):224–31.

[3] Wilson EB, Brooks DG. Translating insights from persistent LCMV infection into anti-HIV immunity. Immunol Res 2010;48(1−3):3–13.

[4] Brooks DG, Trifilo MJ, Edelmann KH, Teyton L, McGavern DB, Oldstone MB. Interleukin-10 determines viral clearance or persistence in vivo. Nat Med 2006;12 (11):1301–9.

[5] Barber DL, Wherry EJ, Masopust D, Zhu B, Allison JP, Sharpe AH, et al. Restoring function in exhausted CD8 T cells during chronic viral infection. Nature 2006;439 (7077):682–7.

[6] Yi JS, Cox MA, Zajac AJ. T-cell exhaustion: characteristics, causes and conversion. Immunology 2010;129(4):474–81.

[7] Zajac AJ, Blattman JN, Murali-Krishna K, Sourdive DJ, Suresh M, Altman JD, et al. Viral immune evasion due to persistence of activated T cells without effector function. J Exp Med 1998;188(12):2205–13.

[8] Jin HT, Anderson AC, Tan WG, West EE, Ha SJ, Araki K, et al. Cooperation of Tim-3 and PD-1 in CD8 T-cell exhaustion during chronic viral infection. Proc Natl Acad Sci U S A 2010;107(33):14733–8.

[9] Zuniga EI, Macal M, Lewis GM, Harker JA. Innate and Adaptive Immune Regulation During Chronic Viral Infections. Annu Rev Virol 2015;2(1):573–97.

[10] Wen J, Elong Ngono A, Regla-Nava JA, Kim K, Gorman MJ, Diamond MS, et al. Dengue virus-reactive CD8(+) T cells mediate cross-protection against subsequent Zika virus challenge. Nat Commun 2017;8(1):1459.

[11] Sullivan NJ, Hensley L, Asiedu C, Geisbert TW, Stanley D, Johnson J, et al. CD8+ cellular immunity mediates rAd5 vaccine protection against Ebola virus infection of nonhuman primates. Nat Med 2011;17(9):1128–31.

[12] Ahmed R, Gray D. Immunological memory and protective immunity: understanding their relation. Science 1996;272(5258):54–60.

[13] Zammit DJ, Cauley LS, Pham QM, Lefrancois L. Dendritic cells maximize the memory CD8 T cell response to infection. Immunity 2005;22(5):561–70.

[14] Bourgeois C, Veiga-Fernandes H, Joret AM, Rocha B, Tanchot C. CD8 lethargy in the absence of CD4 help. Eur J Immunol 2002;32(8):2199–207.

[15] Shedlock DJ, Shen H. Requirement for CD4 T cell help in generating functional CD8 T cell memory. Science 2003;300(5617):337–9.

[16] Sun JC, Bevan MJ. Defective CD8 T cell memory following acute infection without CD4 T cell help. Science 2003;300(5617):339–42.

[17] Jones RB, Ndhlovu LC, Barbour JD, Sheth PM, Jha AR, Long BR, et al. Tim-3 expression defines a novel population of dysfunctional T cells with highly elevated frequencies in progressive HIV-1 infection. J Exp Med 2008;205(12):2763–79.

[18] Tan Z, Zhou J, Cheung AK, Yu Z, Cheung KW, Liang J, et al. Vaccine-elicited CD8+ T cells cure mesothelioma by overcoming tumor-induced immunosuppressive environment. Cancer Res 2014;74(21):6010–21.

[19] Dorhoi A, Du Plessis N. Monocytic Myeloid-Derived Suppressor Cells in Chronic Infections. Front Immunol 2017;8:1895.

[20] Goh CC, Roggerson KM, Lee HC, Golden-Mason L, Rosen HR, Hahn YS. Hepatitis C Virus-Induced Myeloid-Derived Suppressor Cells Suppress NK Cell IFN-gamma Production by Altering Cellular Metabolism via Arginase-1. J Immunol 2016;196 (5):2283–92.

[21] Gabrilovich DI, Nagaraj S. Myeloid-derived suppressor cells as regulators of the immune system. Nat Rev Immunol 2009;9(3):162–74.

[22] Nagaraj S, Collazo M, Corzo CA, Youn JI, Ortiz M, Quiceno D, et al. Regulatory myeloid suppressor cells in health and disease. Cancer Res 2009;69(19):7503–6.

[23] Talmadge JE, Gabrilovich DI. History of myeloid-derived suppressor cells. Nat Rev Cancer 2013;13(10):739–52.

[24] Norris BA, Uebelhoer LS, Nakaya HI, Price AA, Grakoui A, Pulendran B. Chronic but not acute virus infection induces sustained expansion of myeloid suppressor cell numbers that inhibit viral-specific T cell immunity. Immunity 2013;38(2):309–21.

[25] Tacke RS, Lee HC, Goh C, Courtney J, Polyak SJ, Rosen HR, et al. Myeloid suppressor cells induced by hepatitis C virus suppress T-cell responses through the production of reactive oxygen species. Hepatology 2012;55(2):343–53.

[26] Tan Z, Liu L, Chiu MS, Cheung KW, Yan CW, Yu Z, et al. Virotherapy-recruited PMN-MDSC infiltration of mesothelioma blocks antitumor CTL by IL-10-mediated dendritic cell suppression. Oncoimmunology 2019;8(1):e1518672.

[27] Hu CE, Gan J, Zhang RD, Cheng YR, Huang GJ. Up-regulated myeloid-derived suppressor cell contributes to hepatocellular carcinoma development by impairing dendritic cell function. Scand J Gastroenterol 2011;46(2):156–64.

[28] Veglia F, Perego M, Gabrilovich D. Myeloid-derived suppressor cells coming of age. Nat Immunol 2018;19(2):108–19.

[29] Zhou J, Cheung AK, Tan Z, Wang H, Yu W, Du Y, et al. PD1-based DNA vaccine amplifies HIV-1 GAG-specific CD8+ T cells in mice. J Clin Invest 2013;123 (6):2629–42.

[30] Potash MJ, Chao W, Bentsman G, Paris N, Saini M, Nitkiewicz J, et al. A mouse model for study of systemic HIV-1 infection, antiviral immune responses, and neuroinvasiveness. Proc Natl Acad Sci U S A 2005;102(10):3760–5.

[31] Kelschenbach JL, Saini M, Hadas E, Gu CJ, Chao W, Bentsman G, et al. Mice chronically infected with chimeric HIV resist peripheral and brain superinfection: a model of protective immunity to HIV. J Neuroimmune Pharmacol 7(2):380−7.

[32] Dross SE, Munson PV, Kim SE, Bratt DL, Tunggal HC, Gervassi AL, et al. Kinetics of Myeloid-Derived Suppressor Cell Frequency and Function during Simian Immunodeficiency Virus Infection, Combination Antiretroviral Therapy, and Treatment Interruption. J Immunol 2017;198(2):757–66.

[33] Hadas E, Borjabad A, Chao W, Saini M, Ichiyama K, Potash MJ, et al. Testing antiretroviral drug efficacy in conventional mice infected with chimeric HIV-1. AIDS 2007;21(8):905–9.

[34] Liu L, Wei Q, Lin Q, Fang J, Wang H, Kwok H, et al. Anti-spike IgG causes severe acute lung injury by skewing macrophage responses during acute SARS-CoV infection. JCI Insight 2019;4(4).

[35] Saini M, Hadas E, Volsky DJ, Potash MJ. Vaccine-induced protection from infection of mice by chimeric human immunodeficiency virus type 1, EcoHIV/NL4-3. Vaccine 2007;25(52):8660–3.

[36] Roshorm Y, Cottingham MG, Potash MJ, Volsky DJ, Hanke T. T cells induced by recombinant chimpanzee adenovirus alone and in prime-boost regimens decrease chimeric EcoHIV/NDK challenge virus load. Eur J Immunol 42(12): 3243−55.

[37] Cheong C, Matos I, Choi JH, Dandamudi DB, Shrestha E, Longhi MP, et al. Microbial stimulation fully differentiates monocytes to DC-SIGN/CD209(+) dendritic cells for immune T cell areas. Cell 2010;143(3):416–29.

[38] Heath WR, Carbone FR. Dendritic cell subsets in primary and secondary T cell responses at body surfaces. Nat Immunol 2009;10(12):1237–44.

[39] Cervantes-Barragan L, Lewis KL, Firner S, Thiel V, Hugues S, Reith W, et al. Plasmacytoid dendritic cells control T-cell response to chronic viral infection. Proc Natl Acad Sci U S A 2012;109(8):3012–7.

[40] Yu Z, Tan Z, Lee BK, Tang J, Wu X, Cheung KW, et al. Antigen spreading-induced CD8+T cells confer protection against the lethal challenge of wild-type malignant mesothelioma by eliminating myeloid-derived suppressor cells. Oncotarget 2015;6(32):32426–38.

[41] Sammicheli S, Kuka M, Di Lucia P, de Oya NJ, De Giovanni M, Fioravanti J, et al. Inflammatory monocytes hinder antiviral B cell responses. Sci Immunol 2016;1 (4).

[42] Ahmed R, Simon RS, Matloubian M, Kolhekar SR, Southern PJ, Freedman DM. Genetic analysis of in vivo-selected viral variants causing chronic infection: importance of mutation in the L RNA segment of lymphocytic choriomeningitis virus. J Virol 1988;62(9):3301–8.

[43] Mueller SN, Matloubian M, Clemens DM, Sharpe AH, Freeman GJ, Gangappa S, et al. Viral targeting of fibroblastic reticular cells contributes to immunosuppression and persistence during chronic infection. Proc Natl Acad Sci U S A 2007;104 (39):15430–5.

[44] Wherry EJ, Blattman JN, Murali-Krishna K, van der Most R, Ahmed R. Viral persistence alters CD8 T-cell immunodominance and tissue distribution and results in distinct stages of functional impairment. J Virol 2003;77(8):4911–27.

[45] Wherry EJ, Teichgraber V, Becker TC, Masopust D, Kaech SM, Antia R, et al. Lineage relationship and protective immunity of memory CD8 T cell subsets. Nat Immunol 2003;4(3):225–34.

[46] Medzhitov R, Schneider DS, Soares MP. Disease tolerance as a defense strategy. Science 2012;335(6071):936–41.

[47] Mueller SN, Ahmed R. High antigen levels are the cause of T cell exhaustion during chronic viral infection. Proc Natl Acad Sci U S A 2009;106(21):8623–8.

[48] Matloubian M, Kolhekar SR, Somasundaram T, Ahmed R. Molecular determinants of macrophage tropism and viral persistence: importance of single amino acid changes in the polymerase and glycoprotein of lymphocytic choriomeningitis virus. J Virol 1993;67(12):7340–9.

[49] Qin A, Cai W, Pan T, Wu K, Yang Q, Wang N, et al. Expansion of monocytic myeloid-derived suppressor cells dampens T cell function in HIV-1-seropositive individuals. J Virol 2013;87(3):1477–90.

[50] Daley JM, Thomay AA, Connolly MD, Reichner JS, Albina JE. Use of Ly6G-specific monoclonal antibody to deplete neutrophils in mice. J Leukoc Biol 2008;83 (1):64–70.